INVESTIGATION ON SCATTER OF COMPOSITES IN COMPARISON WITH METALLIC MATERIALS

R. Pfaller* / P. Gergely* / A. Weinert**

*Eurocopter Deutschland GmbH, 81663 München
*E-mail: rupert.pfaller@eurocopter.com
**HEAD GmbH, Herzogstr. 1, 80803 München

Keywords: Scatter, fiber, composites, fatigue, Weibull function, shear specimens, bending specimens

Abstract
Today composite materials are typically used for several components in aviation industry. They are especially well known for their excellent fatigue and damage tolerant behavior. Due to the opportunity of load adapted specific fiber layups, it is possible to design more efficient and weight reduced components in contrast to metal parts. But on the other hand, fiber composites are considered with remarkable reduction factors.
Currently, for composite components, the aviation regulations request to reduce the allowable static and dynamic strength because of material scattering, compression after impact, notch sensitivity and hot/wet environmental conditions. Morever, there is often a discussion about the possible high scatter of fiber materials. It is assumed by default that the scatter is higher than that of the metallic materials.
This paper shows the investigations performed with coupon and component test results to determine the scatter of the specimens and the comparison with the mean value. For this purpose the single test results (i.e. data points) are projected to the same number of load cycles. Without the influence of manufacturing deviations, which can be detected by quality inspection measures, the results show similar scatter bands as metallic coupon and component tests.
The outcome of this study can be used as contribution to clarify the discussion on additional reduction factors for the scatter of the fiber reinforced composite material strength.

1 INTRODUCTION

Mainly due to their excellent stiffness and strength to weight ratio, usage of fiber composites is growing since the first all composite airplane, “Sailplane Phönix”, was developed in the 1950s. Serial composite applications in commercial aircraft industry began in the mid of 80’s with a few single airframe parts, such as horizontal stabilizer and vertical fin. Nowadays, about 50% of airframe weight is made up of fiber composites. One of the first composite applications has been the rotor blades of the MBB helicopters. For this application, mainly loaded by centrifugal forces and bending moments, the favorable properties of fibers were used for efficient designs. Due to the special flexibility of glass fiber composites, the discrete hinges for flapping and lead lag motions could be replaced. In the 90’s, the adjustment of the pitch angle was additionally realized by a bearingless design. In contrary to many other parts, rotor blades are extremely loaded by very high dynamic loads.

Since the beginning, the fatigue behavior of the fiber composite materials has been investigated. Besides the testing of laboratory samples in an early development phase and for quality assurance purposes, lots of coupon tests were performed. These samples were directly taken from the rotor blades. Moreover, in the frame of quality assurance, full scale rotor blades have been tested at different areas. So, along the past years, an impressive data base was obtained giving an impression about the scatter of fiber composites [1, 2]. An overview of this data bases is given in this paper, considering as well the other effects like temperature, humidity and damage tolerance.

2 METHODOLOGY OF STATISTICAL ANALYSIS

An appropriate statistical method is necessary to guarantee a certain low probability of failure which is required especially for critical components of the aircraft industry. The failure of a critical component has to be extremely remote. Static strength is assured by A-values for critical parts which guarantee a survival probability of 99% at a confidence level of 95%. Additionally, the so called Limit Load (covering the highest possible load expected during a complete aircraft life) has to be multiplied with the factor of 1.5 at least. This ultimate load has to be substantiated by calculations supported by test results or by test until total failure.
Similar approach has to be followed for fatigue analysis to substantiate an equivalent safety level to ensure that the failure of a part during its lifetime is extremely remote. An equivalent approach for fatigue is the use of so called S/N curves which represent the relation between the strength (S) of a part and number of load cycles to failure. These S/N curves are only valid for a constant stress ratio R. The stress ratio R can be calculated by the following equation:

$$R = \frac{S_{mean} - S_{amplitude}}{S_{mean} + S_{amplitude}}$$

The scatter has to be considered here as well to get the safe or working curve. Such a curve is linked to a certain failure probability, e.g. less than 10^{-9} per hour. The reduction of the mean curve mainly depends on the amount of test specimens and their scatter. Normally many sample tests are performed to determine the

material properties. Usually, fatigue tests at different constant stress levels are performed to determine an S/N curve. Two ranges of an S/N curve are normally distinguished [5]:

- Low cycle fatigue range, which starts below the static failure level and ends at stress levels above the endurance strength. In terms of load cycles, the range is usually positioned between 10^3 or 10^4 until 10^5 or 10^6, which is the span where the curve is inclined. This is shown in Fig. 1 with the red vertical bars between 10^4 and 10^6 load cycles.
- High cycle fatigue range is usually above 10^5 or 10^6. At this span the curve starts to become horizontal (Fig. 1)

Sometimes different reduction factors for the low and high cycle fatigue range are used to determine the save curve. In low cycle fatigue range, it is possible to reduce the curve in horizontal direction and in vertical direction if the inclination is not too high. For the high cycle fatigue range, only a reduction in vertical direction is possible; because a shift in load cycle direction would have no effect on a horizontal line.

Depending on type, size and testability of the critical part, full scale component tests are performed in addition to the basic coupon tests. The number of tested components and scatter of the test results are important to derive the working fatigue curve, which is used to calculate the safe lifetime. In principal, there is no difference between metal and fiber parts in terms of safe life calculations. Furthermore damage tolerance aspects have to be considered as far as possible.

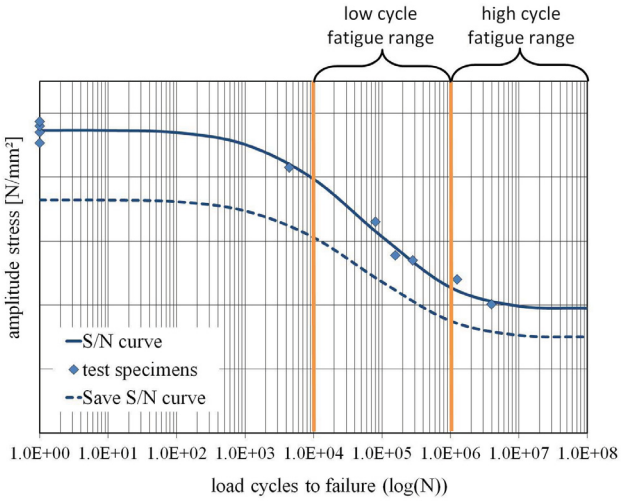

Fig. 1 S/N curve (Weibull curve) showing the relation of failure amplitude stress versus load cycles.

2.1 Mathematical Theory of Fatigue Curve and Statistics

The equation of the four parametric Weibull mean curve is shown below as it is used at Eurocopter Deutschland GmbH (ECD) and plotted in Fig. 1 [1, 2, 4].

The amplitude strength ($S_a(N)$) as a function of load cycles is given as:

$$S_a(N) = S_{a_\infty} + \frac{S_{a_{ult}} - S_{a_\infty}}{e^{\left[\left(\frac{\log(N)}{\alpha}\right)^{\beta}\right]}}$$

S_{a_∞} = Endurance strength (amplitude)
S_{ault} = static strength (amplitude)
N = number of load cycles to failure
α, β = Constants defining the shape of the S/N curve

Contrary to other common fatigue curves, static stress is linked to the dynamic stress with this expression. Consequently, static and dynamic failure is presented in the same consistent equation. Usually stress or load is expressed in amplitude values with respect to a constant stress ratio R.

The so called mean curve according to Fig. 2 is fitted by optimizing the distance to the failure points with the least square method. To take into account the failures at different cycles and load levels, all test points are projected to the 10^0 load cycles along curves with the same shape parameters like the mean curve, as shown in Fig. 2. So, it is possible to consider the relative distance of each point to the curve.

The statistical calculation of the test data for different load cycle ranges is performed according to basic population and random sample for scatter analysis. The analysis of random sample refers only to the test data, which are projected to the same number of load cycles in the chosen load cycle range. It is assumed that the true mean value is unknown. In case of basic population analysis for different load cycle ranges, it is assumed that the true mean value is known and is the same as the mean value of all samples. Of course, this is only correct if many samples are tested. Basically, both methods should lead to similar results. The direct comparison of the results should reveal that the scatter of samples is independent of the number of load cycles to failure and the four parametric Weibull function is well suited to represent the relation of strength and load cycles.

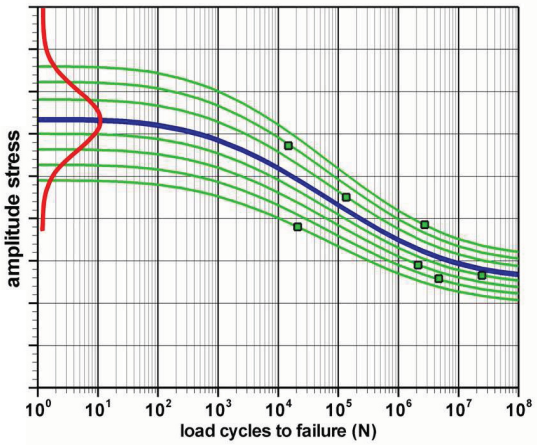

Fig. 2 Projection of the test points along the S/N curve to a single number of load cycles to failure. The red curve shows the distribution of the projected test samples.

The same projection is also used for all other statistic equations.

Mean value μ can be determined as:

$$\mu = \frac{1}{n}\sum_{i=1}^{n} S_{a_i}$$

In case of logarithmic distribution the mean value has to be converted.

Standard deviation is given as:

$$\sigma = \sqrt{\sum_{i=1}^{n} \frac{(S_{a_i} - S_a)^2}{n-1}}$$

Coefficient of variation is defined as:

$$V = \frac{\sigma}{\mu}$$

Logarithmic standard deviation is:

$$\sigma_{log} = \sqrt{\sum_{i=1}^{n} \frac{(\log((S_{a_i})) - \log(S_a))^2}{n-1}}$$

Finally the "Scatter factor" can be calculated as:

$$\varepsilon = 10^{\sigma_{log}}$$

Calculation of the reduction factors

ECD distinguishes between four different reduction factors determined by:

- Symmetrical normal distribution of random sample (population unknown)

$$j = \frac{\mu - k \cdot \sigma}{\mu}$$

$$k = \frac{2(n-1)}{2(n-1) - a'^2}\left[a + \frac{a'}{\sqrt{2(n-1)}} \cdot \sqrt{\frac{2(n-1)}{n} + a^2 - \frac{a'^2}{n}}\right]$$

n...number of specimens

$a = 4.75059$ (for survival probability of 99.9999%)

$a' = 1.64521$ (for confidence level of 95%)

- Symmetric normal distribution of basic population (known population)

$$j = \frac{1 - a \cdot V}{1 + a' \cdot \left(\frac{V}{\sqrt{n}}\right)}$$

- Reduction factor for logarithmic normal distribution of random sample (population unknown)

$$j = \frac{1}{\varepsilon^k}$$

- Logarithmic normal distribution of basic population (known population)

$$j = \varepsilon^{-\left(a + \frac{a'}{\sqrt{n}}\right)}$$

3 SCATTER OF TEST SPECIMENS FOR DIFFERENT MATERIALS

3.1 E-Glass Fiber Composite (GFC) Shear Specimens

Short bending specimens are used to determine the interlaminar shear strength (τ_{ils}) of fiber reinforced composite materials (Fig. 3). The test specimens cut from serial BO105 main rotor blades, which are made of GFC wet laminate Tex-Roving with LY556-HT972 resin, are evaluated in this chapter. In total 76 fatigue specimens are tested at a stress ratio of R= 0.111. Fig. 3 shows the test setup. The short bending or shear specimen is positioned on two supports and loaded by a vertical dynamic force "F" in the middle. The parameter l_v (distance between two supports) has been chosen in such a way that the ratio between the resulting bending and shear stresses in the laminate is less than 10. This is achieved for small l_v and explains why the test is called also short bending test (known with the name Amsler Test as well). This ratio guarantees that a shear crack will occur and that the influence of bending can be neglected [3].

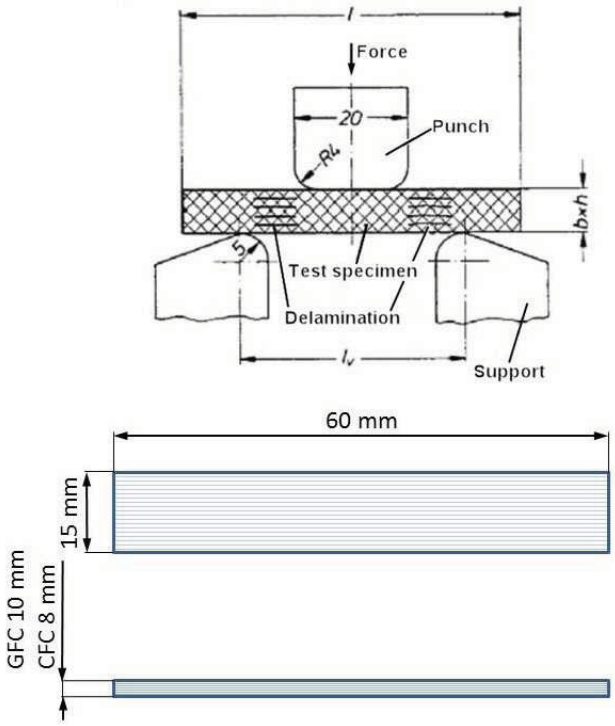

Fig. 3 Test setup and geometry of the of GFC shear specimens ("Amsler Test")

Fig. 4 shows the test results and the resulting S/N curve. As described in Chapter 2.1, the S/N curve is determined by linear regression analysis based on the least square method. The asymptotic high cycle fatigue range is reached at approximately 1 Mio load cycles to failure (log(N) = 6) [6].

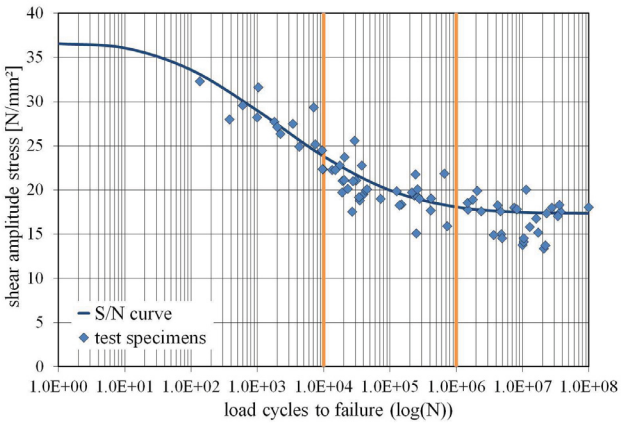

Fig. 4 S/N curve of E-Glass Fiber Composite (GFC) shear specimens at stress ratio of R= 0.11 (fiber volume ratio V_f = 57%)

The scatter of the test points is nearly constant over the complete range of load cycles as it is shown in Table 1. One reason for the scatter is the high amount of blades and different areas from where the samples are cut. The cutting process itself has also an influence on the scatter. Fiber composite materials are very sensitive to the load direction. If the cut is not exactly parallel to the fiber direction, test results may diverge considerably. Usually, fiber composite materials loaded in transverse fiber direction show higher scatter since the many interfaces between ply layers are concerned. Composites loaded in fiber direction have redundant load paths. Therefore, as shown in the next example, the scatter of unidirectional bending specimens is low. For the full scale component, it is also a good design practice to avoid a critical load path related to matrix failure. Examples for these two different failure modes for a full scale component are given in chapter 4.

			N° of tests	Mean value	Standard deviation	Scatter factor
			[-]	[log(MPa)]	[log(MPa)]	[MPa]
$1<N<\infty$	Log. normal distribution	Basic population	85	1.563	0.044	1.105
		Random sample	85	1.548	0.041	1.099
$10^4<N<10^6$	Log. normal distribution	Basic population	33	1.563	0.043	1.104
		Random sample	33	1.549	0.040	1.098
$10^6<N<\infty$	Log. normal distribution	Basic population	28	1.563	0.055	1.135
		Random sample	28	1.542	0.051	1.123

Table 1 Statistics of the test data of E-Glass shear specimens for the different load cycle ranges as shown in Fig. 4.

3.2 E-Glass Fiber Composite Bending Specimens

The long bending test specimens are used to determine the tensile and compressive strength of fiber reinforced composite materials. The samples cut from serial BO105 main rotor blades, which are made of GFC wet laminate Tex-Roving with LY556-HT972 resin, are evaluated here. In total 131 specimens were tested at a stress ratio of R= 0.2. The samples have been tested within the scope of so called quality assurance tests. After a certain production rate, besides some full scale component tests, samples directly cut out of some areas of the blades are tested additionally.
The test setup, as shown in Fig. 5, is similar to the GFC shear specimens (Chapter 3.1). The main difference is the higher distance between the supports and the larger load punch. Due to the chosen distance of 160 mm between the supports, the relation of bending to shear stress is larger than 50. Thus, the shear stress in the laminate can be neglected and bending cracks will occur [3].

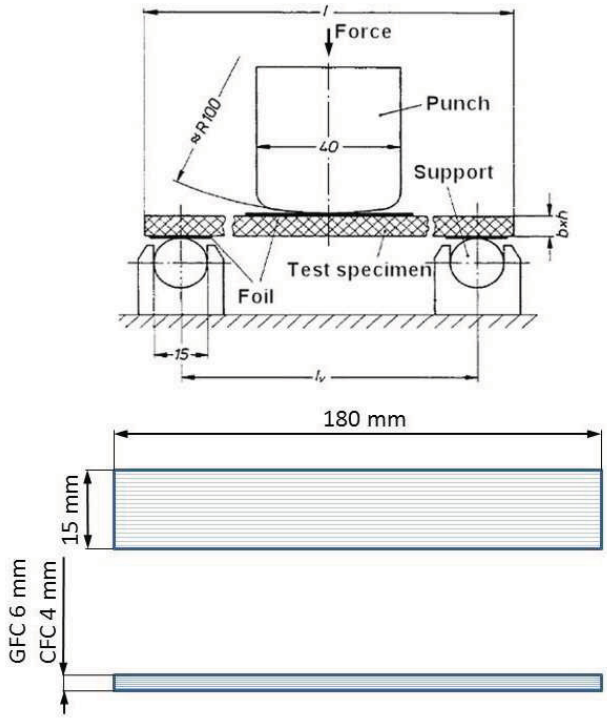

Fig. 5 Test setup and the geometry of GFC bending specimens (“Schenck Test”)

Fig. 6 shows the S/N curve of the GFC bending specimens with test points. Four parametric Weibull curve is used as well to create the S/N curve. The asymptotic range of the endurance limit is reached at 100 Mio load cycles to failure (log(N) = 8). The scatter is almost constant over the complete range of load cycles (see Table 2). Similarly, the main reason for the scatter is the amount of blades and the different areas from where the samples are cut. The cutting process itself has also an influence [6].

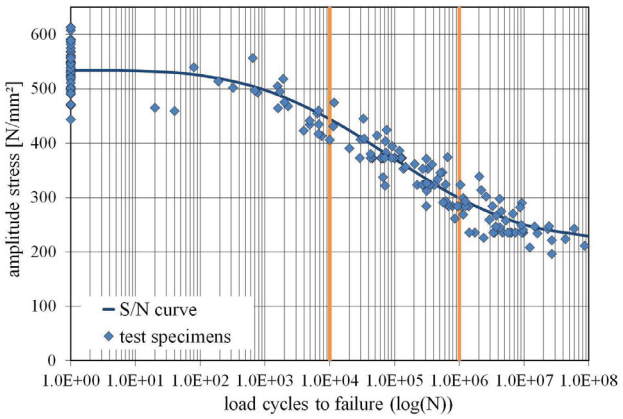

Fig. 6 S/N curve and test data of E-Glass specimens at stress ratio R= 0.2 (fiber volume ratio V_f = 57%)

			N° of test points	Mean Value	Standard deviation	Scatter factor
			[-]	[log(MPa)]	[log(MPa)]	[MPa]
1<N<∞	Log. normal distribution	Basic population	179	2.728	0.034	1.083
		Random sample	179	2.721	0.034	1.081
10^4<N<10^6	Log. normal distribution	Basic population	62	2.728	0.031	1.073
		Random sample	62	2.723	0.030	1.072
10^6<N<∞	Log. normal distribution	Basic population	46	2.728	0.043	1.104
		Random sample	46	2.714	0.041	1.098

Table 2 Statistics for the test data of E-Glass bending specimens

3.3 R-Glass Fiber Composite (GFC) Bending Specimens

Fig. 7 shows the R-Glass/Epoxy bending test specimens and the corresponding S/N curve. Laboratory samples have been tested with the same test set up as shown in Fig. 5. However, for these test samples the width of the specimen was 10 mm instead of 15 mm and the thickness was increased to obtain the same bending stiffness as the original geometry. In this case, the scatter is high and the static strength seems to be low for the R-Glass material.

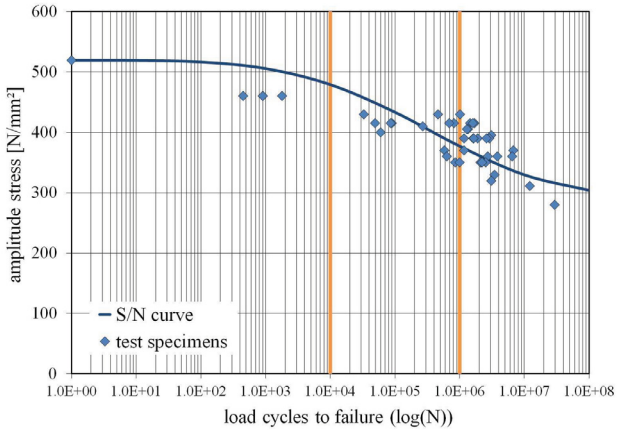

Fig. 7 S/N curve and test data of R-Glass specimens at stress ratio R= 0.2 (Sample width of 10 mm).

The same test was performed with the original sample geometry as shown in Fig. 5. The results are presented in Fig. 8. Even with a less number of test samples, it is obvious that the scatter is reduced considerably and also the static strength is increased as expected.
The explanation for this effect is that the sample with the smaller width and increased thickness is loaded by higher compression at the location of the load introduction. At this area, fibers are damaged leading to a locally reduced strength. Then, at least a part of the cross section is destroyed. This results not only in a lower static and fatigue strength but also in higher scatter.

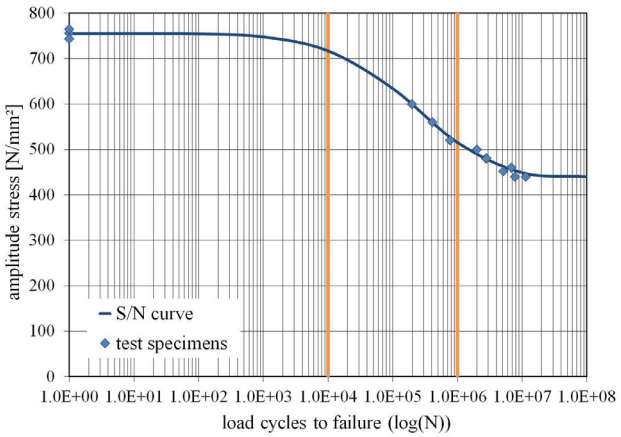

Fig. 8 S/N curve and test data of R-Glass specimens at stress ratio R= 0.2 (sample width of 15 mm).

Another example for a similar effect is presented in Fig. 9. Here, same kind of samples is tested in bending. Normally, a thin KAPTON foil is positioned between the sample and the load introduction punch. Leaving away the KAPTON foil causes damages as a result of introduced pressure in combination with friction. The effect of the poor load introduction on scatter can be seen in Fig. 9 below. The specimens without KAPTON foil are marked with green points. It is obvious that not only the static and fatigue strength of those samples are reduced but also the scatter is increased considerably. These results would lead to very low endurance values. With KAPTON foil, a higher and realistic strength value is obtained with a small scatter band. These examples show that it is very important to take a lot of care over the selection of the right specimen types and test conditions. Otherwise unrealistic low strength results could be obtained independently from the real material strength.

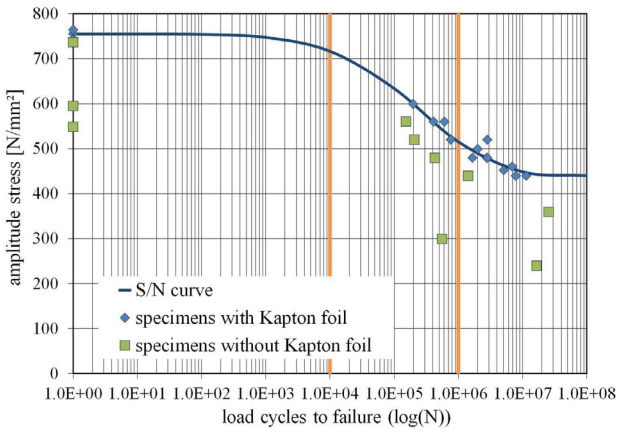

Fig. 9 S/N curve and test data of R-Glass specimens at stress ratio R= 0.2 (sample width of 15 mm).

3.4 Rotating Bending Specimens of 1.4545.3 Steel

Rotating bending specimens cut from the main rotor shaft of the EC135 helicopter is considered here. These test results are used to determine the influence of the nickel coating on fatigue strength as well. The material of the specimens is steel 1.4545.3. In total 45 specimens have been tested; 21 specimens without coating and 24 with coating. The chemical nickel coating on each specimen is app. 25 µm thick. The shape of the specimen is shown in Fig. 10.

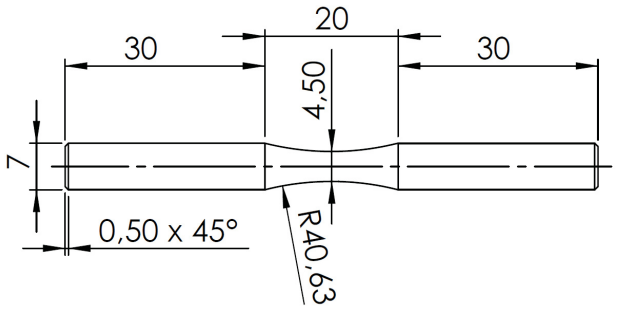

Fig. 10 Shape of the rotating bending specimens

The results are shown in Fig. 11 as amplitudes versus load cycles. The range of high and low cycle fatigue is separated with the red vertical lines in the diagram.

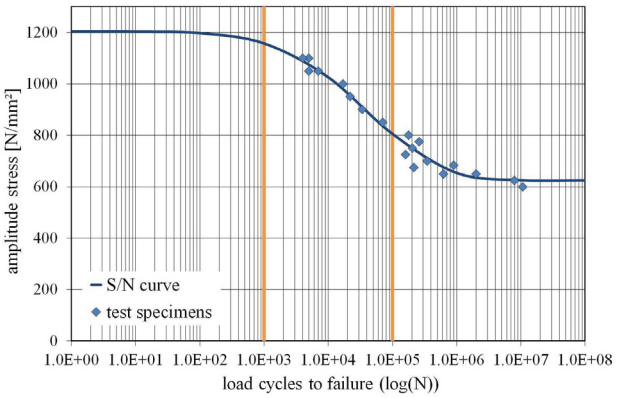

Fig. 11 S/N curve and test data of steel 1.4545.3 bending specimens (R= -1)

In Table 3 the statistical results of the fatigue test data are given. Above 10^5 load cycles, which is the border line between high and low cycle fatigue, the scatter increases. This is directly visible in the diagram in Fig. 11. This might be caused by some effects which are typical for metals under high cycle fatigue loads such as notch sensitivity and corrosion fatigue. Some other effects like fretting can be excluded for laboratory samples.

			N° of test points	Mean value	Standard deviation	Scatter factor
			[-]	[log(MPa)]	[log(MPa)]	[MPa]
$1<N<\infty$	Log. normal distribution	Basic population	19	3.080	0.016	1.039
		Random sample	19	3.080	0.016	1.039
$10^3<N<10^5$	Log. normal distribution	Basic population	8	3.080	0.007	1.017
		Random sample	8	3.081	0.007	1.017
$10^5<N<\infty$	Log. normal distribution	Basic population	11	3.080	0.021	1.050
		Random sample	11	3.079	0.021	1.050

Table 3 Statistics for the rotating bending specimens of steel 1.4545.3

Similar behavior is also presumable for some surface treatments as it can be seen clearly in Fig. 12. This figure shows the same material with nickel plating. Even the static and endurance strength is slightly increased; the negative effect on scatter is much higher. Also, the progression of scatter in the direction of higher load cycles is noticeable. This would lead to a higher reduction factor for the safe material fatigue stress curves especially at higher load cycles. Therefore the part would have to be dimensioned with high reserve factors compared to the mean endurance strength. Considering samples of an unknown population, the reduction factors for the endurance strength of samples with and without nickel plating are:

Without nickel plating	0.692 [-]
With nickel plating	0.325 [-]

This gives an impression of many different high cycle fatigue aspects associated to metallic materials, which will be even more severe when the in service effects like fretting and corrosion are considered.

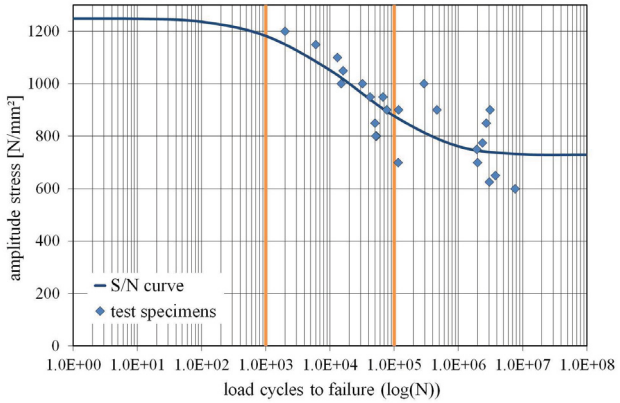

Fig. 12 S/N curve and test data of steel 1.4545.3 bending specimens with nickel coating (R= -1)

4 COMPONENT TESTS

4.1 Flexbeam of EC135 Main Rotor Blade

During the development phase and also during production, critical areas of the main rotor blades have to be tested. After a certain production rate, full scale blades are tested to ensure the quality of the manufacturing. Therefore, several test data exist compared to other components. So far 23 flexbeams have been tested. Flap and lead-lag bending moments are applied to the test parts at the attachment/root area as shown in Fig. 13. The area with the highest curvature in Fig. 13 represents a virtual flapping hinge which replaces the discrete mechanical hinges in conventional designs. As a result of the bending moments, a torsional moment at the root area occurs due to the flap/lead-lag coupling. Two failure modes are obvious: Fiber cracks at the most critical loop area at the root and horizontal delaminations developing through the flapping hinge area.

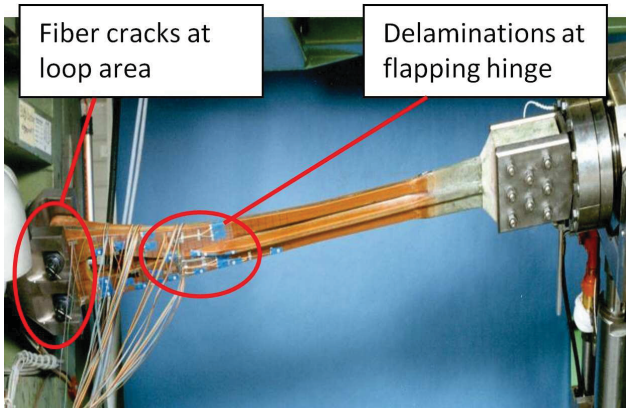

Fig. 13 EC135 Flexbeam bending test

Similar to the coupon tests, an S/N curve was created with the test points. All points are shown together in one diagram in Fig. 14. As shown in this figure, some parts fail in delamination before the mean curve is reached. This failure mode is considered as uncritical, because the main functions and the safety of the main rotor blade are still not affected. If this failure mode is considered together with the loop failure, the level of scatter increases. A scatter factor of 1.068 for a random sample is calculated based on log normal distribution. It is expected that this kind of failure will become evident by an increased vibration level.

The more critical failure mode is the fiber crack at the loop area. Therefore, it makes sense to treat both failure modes with different criterions concerning the reduction factors for the safe S/N curve which is used to calculate the safe life of the part [4, 5].

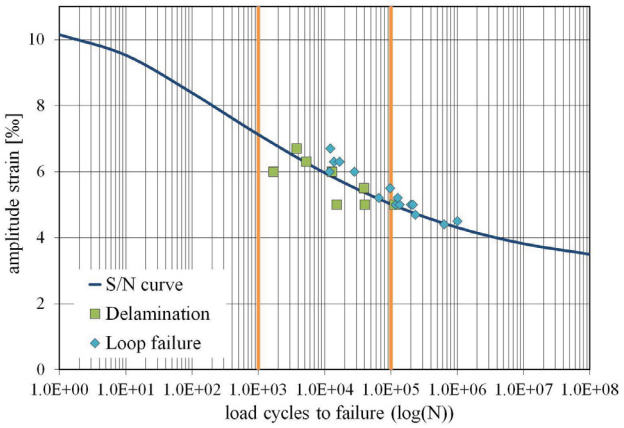

Fig. 14 S/N curve and test data of the Flexbeam component test for the loop failure and delamination failure modes (R= -0.24)

Flexbeam Loop Failure

To consider only the critical failure mode, delamination failures have been removed and a new S/N curve is optimized through the test points. As a result, the curve is shifted upward to higher loads and cycles. Also the scatter is reduced from 1.068 to 1.036. So, based on the critical fiber failure mode, a very low scatter is obtained.

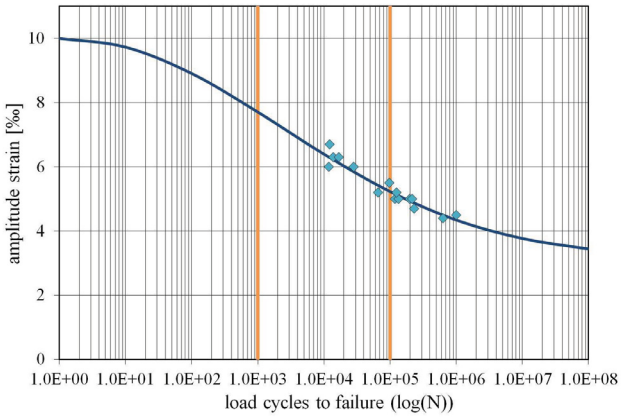

Fig. 15 S/N curve and test data of the EC135 Flexbeam component test for loop failure mode (R= -0.24)

To interpret the test results of this part in a correct way, a few more facts have to be considered:

- As test articles, components with poor quality are often used in the frame of quality assurance and sometimes of development phase. One reason is to cover intrinsic damages and to ensure the safety of parts for the complete range of the production quality. Intrinsic damages means intrinsic or discrete imperfections or flaws related to manufacturing operations, processes or assembly such as voids, gaps, porosity, inclusions, fiber dislocation, disbonds, and delaminations. Another reason is to cover occurring phenomena for which the available knowledge seems to be insufficient.
- There is a natural crack arrest for the loop area when the crack reaches the middle of the cross section. For the EC135 main rotor blade, the test is stopped when a quarter of the lug area has

failed. The horizontal shear web in this area acts as a crack stop. So, for this main rotor blade the fatigue point in the S/N curve is directly linked to the failure of the part. For other designs with only one lug the test is not always stopped at the failure of the part because, the test set up could be damaged. Therefore, a certain stiffness deviation (about 10%) or a certain crack length is used as failure criteria to stop the test.

- According to the existing regulations, a residual strength test has to be performed at the end of the fatigue test with limit or ultimate load by including the effects of temperature and humidity. Therefore, fatigue test has to be stopped before the final failure of the part. Due to its high fatigue capacity and normally slow crack growth rate, this is not a problem for this component even when one quarter of the lug has failed. Therefore, the scatter is defined by the failure of the part.

			N° of tests	Mean value	Standard deviation	Scatter factor
			[-]	[log(‰)]	[log(‰)]	[‰]
$1<N<\infty$	Log. normal distribution	Basic population	15	1.00	0.015	1.036
		Random sample	15	1.00	0.015	1.036
$10^3<N<10^5$	Log. normal distribution	Basic population	7	1.00	0.020	1.046
		Random sample	7	1.01	0.019	1.044
$10^5<N<\infty$	Log. normal distribution	Basic population	8	1.00	0.012	1.027
		Random sample	8	1.00	0.012	1.027

Table 4 Statistics of the EC135 Flexbeam component test results for loop failure

Scatter is very low for this part especially when it is considered that it is not a small specimen but a complex component. The values are shown in Table 4. The complete range of cycles is considered in this table. But also the difference between the high and low cycle fatigue range, for which the threshold is assumed as 10^5 load cycles, is distinguished. Symmetrical and log normal distribution show nearly the same scatter for all ranges. There is also a small difference between high and low cycle fatigue. Nevertheless, a minimum scatter is assumed to calculate the reduction factor for the safe fatigue curve.

Several factors, as mentioned above, have an influence on the scatter of the test components and on the shape of the S/N curve. Therefore, it is more difficult to get the scatter of real strength of a component compared to coupon tests.

The flexbeam delamination alone is not considered because it is based on a different load type (interlaminar shear stress τ_{ils} instead of normal stress σ) and the failure in delamination is assumed to be uncritical as mentioned. Therefore, this failure mode has to be considered only for reliability aspects with smaller reduction factors (uncritical failure).

4.2 Consequences of Delamination as an Example for the Crack Growth at BK117 Main Rotor Blade Loop

Another example for the effect of delamination is shown below for the fatigue test performed on BK117 main rotor blade loop area at the blade root end (see Fig. 16).

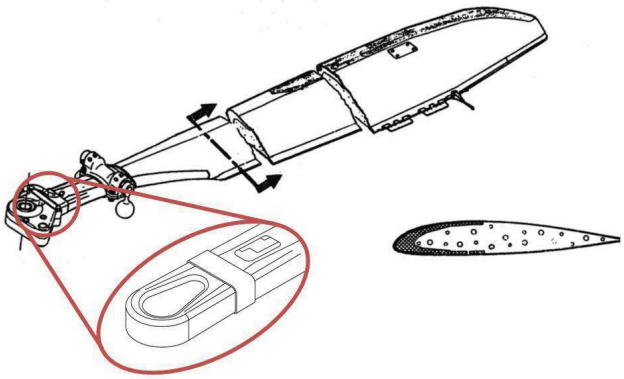

Fig. 16 BK117 main rotor blade with the loop area

This test was performed to determine the crack growth at this area. The results are presented in Fig. 17. There are three curves in this diagram. Two curves for the delamination growth, the vertical and the horizontal ones, and the one for the crack growth. The blade was dynamically tested with a constant amplitude load. As it is apparent, the crack growth (bottom curve) is nearly constant approximately until the half of the cross section area is broken. Afterwards, for the same number of load cycles, there is almost no crack growth but delaminations in both directions are propagating. The reason for this behavior can be explained as follows: A natural discontinuity in the middle of the cross section in horizontal plane is introduced during the manufacturing of the blade. When the crack reaches this area, the complete half of the cross section starts to delaminate. But the crack growth stops for a long time. After the stop, new crack starts at the second half of the cross section. Therefore, it can be stated that under certain circumstances delamination works as a crack arrest on fiber composites.

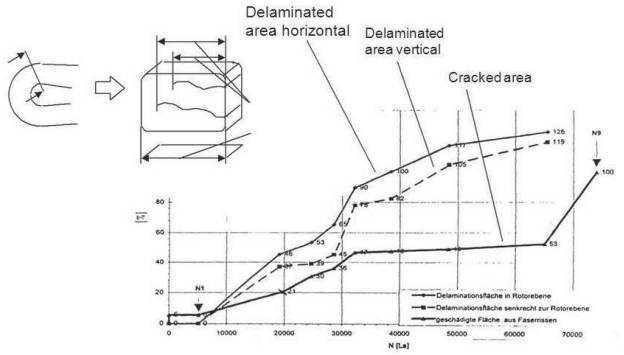

Fig. 17 Loop area delamination and crack growth at the BK117 main rotor blade root end

4.2.1. EC135 Carbon Composite Tail Rotor Drive Shaft

Besides rotor blades, it is beneficial to design some other parts of the helicopter by using fiber reinforced composite materials. For instance, a part of the tail drive shaft can be designed in composite to a certain weight and stiffness ratio, which could be important for dynamic reasons (Figure 18). As for most carbon fiber reinforced parts, impact followed by compression loading is the dominating damage mode for this part as well. Therefore, such damage is applied before each fatigue test. Impacts from 5 J to 25 J have been applied to check the visibility. But only inside the shaft an effect of the impacts has been observed.

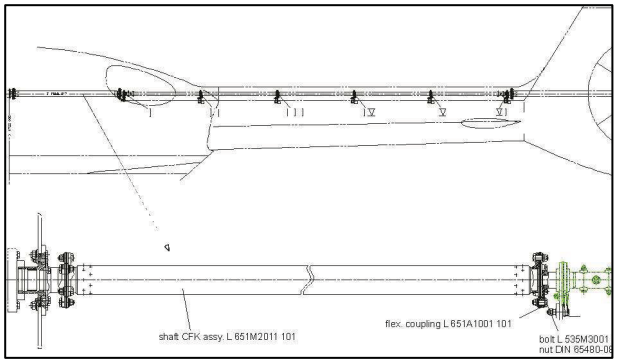

Fig. 18 EC135 carbon composite tail rotor drive shaft

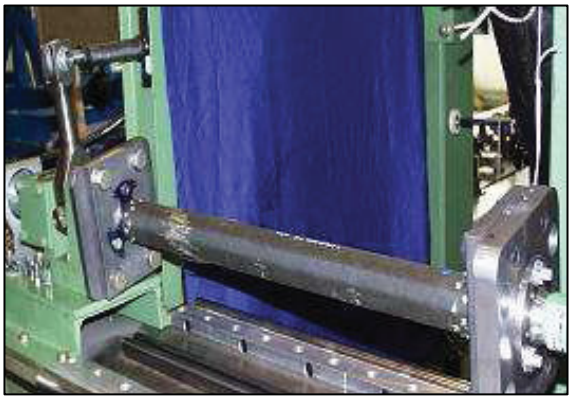

Fig. 19 EC135 carbon composite tail rotor drive shaft on test set-up

Hence, the cut off level of 25 J has been used for the three impacts as shown at Fig. 19. On carbon fiber composite parts the influence of such impacts on the static strength is considerable as it is well known. But as it is known from coupon tests, as soon as there are peak stress effects on carbon parts due to notches or due to poor clamping (see also [3]), the fatigue S/N curve is almost horizontal. This means that the endurance strength is close to the reduced static failure.

At the end of each fatigue test, a residual strength test at ultimate load level by considering additionally the influence of humidity and temperature was performed. Ultimate load was chosen because this part showed no sign of fatigue damage, which could be used as a typical feature for an inspection interval. This is proposed for the parts unsuitable for damage tolerance concepts according to the certification requirements for composite helicopter components.

Static failure in conjunction with impact damage is the dominating critical load case for the tail drive shaft. In practice the use of the component has to be stopped before fatigue failure occurs. Since the fatigue life of this carbon part is assumed to be very high or unlimited, depending on the test load, test is stopped when the component reaches certain number of load cycles which guarantee sufficient fatigue life without fatigue damage. This is shown in Fig. 20 below. The lower curve is the so called safe S/N curve. Mean curve above is reduced depending on the number of test samples and scatter. As it is obvious, there is no scatter for the fatigue points because the test is stopped artificially when it reaches the predefined amount of load cycles.

As explained in chapter 2 the used form of the S/N curve combines the static failure (at $N = 10^0$) with the fatigue strength. So, for this component it is more reasonable to use the scatter of the static failure. Except one point with lower impact energy the static failure shows a low scatter.

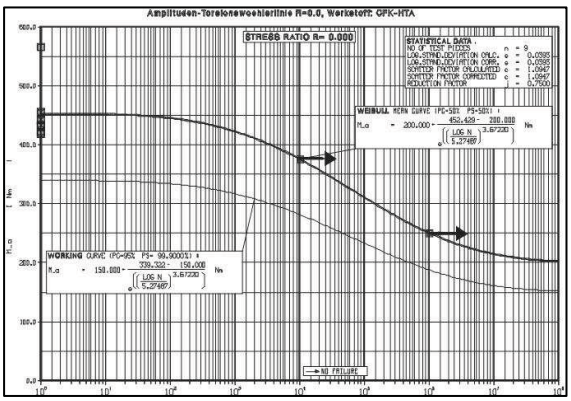

Fig. 20 S/N curve of the EC135 carbon tail rotor drive shaft

5 CONCLUSION

It has been understood that scatter in fatigue tests are very sensitive to test set up, sample configuration and the way of evaluation. Good as well as poor fatigue behavior of composite materials can be demonstrated by sample tests. Unexpectedly low static and fatigue values in combination with a high scatter are often indicating that most probably something went wrong with the tests. Even assumable negligible influences like a thin foil on top of the tested part can have an impressive influence on the scatter and stress level of fatigue curves.

Contrary to metals, for composites from beginning on, several special damaging causes have been defined, such as temperature, humidity, impacts, delamination growth and all possible intrinsic manufacturing defects. All of them generate usually a reduction factor and often all have to be applied at the same time to the same critical area of the component. Regardless if they result in real critical behavior, as it is often not the case. This has been demonstrated with the example of delaminations at loop area of a main rotor blade.

It is shown that for metals there exists sometimes a high scatter which is a result of the material behavior and not the result of a poor test set up or specimen.

The outstanding fatigue behavior of carbon fiber components demonstrate, that a conventional reduction factor based on fatigue failure is not always suitable. The reason is that the endurance strength is close to the static failure and therefore the most important test object is the residual strength test at the end of the fatigue test. For some lay-ups, the static strength after fatigue loading is higher than before.

As conclusion, it can be stated that no extra fatigue factor for composites is needed. But a much differentiated methodology which takes care of each failure mode and its criticality alone is necessary. Together with a good destructive and nondestructive quality control we can make beneficial use of the great fatigue and damage tolerance behavior of composite materials.

REFERENCES

[1] Jarosch, E., Stepan, A.: „Fatigue Properties and Test Procedures of Glass Reinforced Plastic Rotorblades“, American Helicopter Society, 25th Annual National Forum, 1969, Paper No. 370

[2] Och, F.: „Fatigue Strength“, AGARDograph No 292, Helicopter Fatigue Design Guide, Nov. 1983, ISBN 92-835-0341-4

[3] Bansemir, H.: “Prüfmethoden und Prüflingsgestaltung für die Dimensionierung von Faserverbund-strukturen”, Jahrestagung der DGLR, Aachen 2009

[4] Bansemir, H., Emmerling, S.: “Fatigue Substantiation and Damage Tolerance Evaluation of Fibre Composite Helicopter Components“, Applied Vehicle Technology Panel: Applications of Damage Tolerance Principles for Improved Airworthiness of Rotorcraft, Corfu, Greece, 21-22 April 1996

[5] Emmerling, S.: “New Fatigue and Damage Tolerance Evaluation Rules – Are we fit for them?“ 37th European Rotorcraft Forum in Vergiate/Callarate, Italy, Sept. 13-15, 2011

[6] Weinert, A., Gergely, P.: “Fatigue-Strength Surface – Basis for Structural Analysis under Dynamic Loads”, DLRK-2011, Bremen, Sept. 27-29, 2011; Springer Verlag